Analytical Modeling and Optimization of Micro-piezoelectric Energy Harvesting Devices

Mohammed A Al-Ajmi
Mechanical Engineering Department
Kuwait University
P.O. Box 5969, Safat 13060, Kuwait
E-mail: malajmi@kuc01.kuniv.edu.kw

***Abstract* — This work provides an exact analytical dynamics of a cantilever beam bonded with a piezoelectric patch to extract the modal frequencies under open circuit and short circuit electrodes' conditions. The modal open circuit and short circuit frequencies are then used to calculate the corresponding modal Electro-Mechanical Coupling Coefficient (EMCC), which is considered as an influential parameter in the design of piezoelectric based devices such as energy harvesters and smart structures. A parametric analysis is then performed to optimize the length and the thickness of the piezoelectric patch for maximum modal EMCC.**

***Index Terms* — beam, energy harvesting, optimization, piezoelectric, vibration.**

I. INTRODUCTION

Piezoelectric materials have been the focus of intensive research efforts over the last few decades due to their superior electromechanical behavior. These materials are widely used in many engineering applications as sensors, actuators. In the past few years, the demand on piezoelectric based energy harvesters that can perform as miniature self-contained power supplies has highly increased due to the advancement in integrated circuit technology [1]. A crucial performance factor of a vibration based piezoelectric energy harvester is the so called modal Electro-Mechanical Coupling Coefficient (EMCC). The modal EMCC is a ratio that relates the amount of electric energy developed by the piezoelectric material to the total elastic energy of the vibrating structure at some known mode. To determine the modal EMCC, the free vibration problem of the piezoelectric structure should be solved for both Open Circuit (OC) and Short Circuit (SC) electrode conditions. Due to the sensitivity of the EMCC to OC and SC modal frequencies, accurate determination of those frequencies is mandatory.

Examples of early efforts in analytical modeling of piezoelectric beam structures are the works by Bailey and Hubbard [2], Crawley and Luis [3], and Hagood et al [4]. Numerical modeling of piezoelectric structures, which is not the subject of this paper, has received also a great attention for all types of structures as reviewed by Benjeddou [5]. Tong and Luo [6] derived the equations of motion from partial differential forms for a thin piezoelectric smart beam. In their work, exact dynamic solutions, including peel stress, were obtained by using a time-separable solution. In a recent work, Erturk an Inman [7] derived a distributed parameter model for a thin cantilevered beam fully covered with a piezoceramic layer. The equations of motion were obtained for general transient base motion with separate damping coefficients defined for both internal material damping and external air damping. The analytical solution was developed for the coupled electromechanical equations under the common assumption of constant electric field across the piezceramic layer. Maurini et al [8] used enhanced assumed modes with special jump functions that account for material discontinuities between the segments of stepped piezoelectric beam. Their natural frequencies were compared with the exact ones obtained by finding the roots of the dynamic stiffness matrix equation. Burmann et al [9] derived a closed-form, time-separable solution for a cantilever beam partially covered with symmetric piezoceramic layers. Their fully-coupled analytical model counted for the higher order electric field in the piezoelectric material through Gauss law of electrostatics. Bsak et al [10] extended the last mentioned work to asymmetric case where a single piezoceramic layer partially covers the cantilever beam. Maxwell and Asokanthan [11] used the time-separable solution to obtain exact modes and natural frequencies of thick beams with multiple distributed actuators but without inclusion of any active piezoelectric properties. Although exact, time-separable analytical solutions are useful for simple structures, but they get really involved for complex structures due to the large number of unknowns.

Another way of finding a closed form dynamic solution is the transfer matrix method [12]. In this method, a spectral transfer matrix is formulated for one segment (cell) of the distributed parameter system for which the input and output vectors are made of both kinematical variables and internal forces. In the vicinity of active structures, Baz [13] introduced the concept of transfer matrix for periodic spring-mass systems controlled by piezoelectric actuators, and his work has been extended to active and passive control of periodic rods with piezoelectric actuators [14]. However, for structures made of many cells, the transfer matrix of the whole structures is found by chain product of those for the unit cells, which may result in significant round-off errors [15]. Yang and Tan [16] developed a special scheme to determine closed-form transfer functions for distributed parameter systems.

In this work, the DTF will be developed for a cantilever beam, partially covered with a single piezoelectric patch to determine the OC and SC modal frequencies, hence the modal EMCC. A simple extension of the DTF for beams with multiple piezoelectric patches is performed, and the model is validated with the exact solution. A parametric analysis is finally done to optimize the size of the piezoelectric patch.

II. MATHEMATICAL MODELING

Consider a thin elastic beam, with one surface bonded piezoelectric patch, divided into three regions as shown in Fig. 1. The first and last regions are made only of an elastic material while the second one additionally contains a piezoelectric layer completely covering the elastic one. The Euler-Bernoulli in-plane strain is given by

$$\varepsilon_1 = u' - zw'' \tag{1}$$

Where u and w are the in-plane and transverse deformation, respectively, and the number of primes denote the number of differentiation with respect to the x coordinate. The constitutive equations for the piezoelectric beam are

$$\begin{aligned} \sigma_1 &= C_{11}^E \varepsilon_1 - e_{31} E_3 \\ D_3 &= e_{31}\varepsilon_1 + \in_{33}^{\varepsilon} E_3 \end{aligned} \tag{2}$$

Where σ, E and D denote, respectively, the stress, electric field and electric displacement, while e, C and $\in$ stand for the piezoelectric, elastic, and dielectric constants, all in reduced form. Also, superscripts E and ε represent properties measured at constant electric field and constant strain, respectively.

The electric field is defined from the electric potential φ by

$$E_3 = -\varphi_{,3} \tag{3}$$

Where subscript ,3 stands for differentiation through the thickness (3 or z) direction. Gauss' law of electrostatics for a dielectric states that

$$D_{3,3} = 0 \tag{4}$$

The electric boundary conditions are introduced through the potential difference between electrodes, V, such that

$$\varphi\left(\kappa + t_p\right) - \varphi\left(\kappa\right) = \mathrm{V} \tag{5}$$

Substituting the strain and electric field definitions in the electric displacement, applying (4), and using the electric boundary conditions, the electric potential can be found [17], from which the electric field is determined by (3) to be

$$E_3 = -\mathrm{V}/t_p - \left(\alpha - z\right)(e_{31} / \in_{33}^{\varepsilon}) w_{xx} \tag{6}$$

Where $\alpha = \kappa + t_p / 2$ is the distance from the composite's neutral axis to the mid-plane of the piezoelectric layer. Note that the electric field is made of two components: the usually assumed potential difference over the thickness, and the induced electric field due to the deformation of the beam, which will contribute to the flexural rigidity of the beam as will be seen later.

To derive the governing equations of motion for the middle section, Hamilton's principle is first applied

$$\int_{t_1}^{t_2} (\delta T - \delta H + \delta W)\, dt = 0 \tag{7}$$

Where, δH is the virtual electric enthalpy of the thin piezoelectric beam defined on the volume V by:

$$\begin{aligned} \delta H = \int_V (&\delta\varepsilon_1 C_{11}^E \varepsilon_1 - \delta\varepsilon_1 e_{31} E_3 \\ &- \delta E_3 e_{31}\varepsilon_1 - \delta E_3 \in_{33}^{\varepsilon} E_3)\, dV \end{aligned} \tag{8}$$

In addition, δT is the virtual kinetic energy given by:

$$\delta T = \int_V m(\delta\dot{u}\, u + \delta\dot{w}\, \dot{w})\, dV \tag{9}$$

Where m denotes the total mass of both layers per unit length. Assuming no external forces , the virtual work is done only by the electric potential and point charge q on the surface S such that

$$\delta W = -\int_S \delta\varphi\, q\, dS \tag{10}$$

Applying the previous variations and collecting relevant terms, the following set of mechanical equations are obtained

$$\begin{aligned} m\ddot{u} - ku'' &= 0 \\ m\ddot{w} + dw'''' &= 0 \end{aligned} \tag{11}$$

$$m = \rho_b t_b + \rho_p t_p, \qquad k = E_b t_b + C_{11}^E t_p$$

$$d = E_b \overline{I}_b + C_{11}^E \overline{I}_p + (e_{31}^2 / \in_{33}^{\varepsilon}) I_p$$

With ρ, A and E denoting the density, cross section area and Young's modulus of elasticity in longitudinal direction, respectively. Subscript b represents quantities for the beam layer while those for the piezoelectric layer are represented by p. Also $I_i = t_i^3 / 3$ $(i = b,p)$ is the moment of inertia of layer i about its own mid-plane and $\overline{I}_i$ is the inertia of that layer about the composite's neutral axis, which is given for both layers by

$$\overline{I}_b = \kappa t_b(\kappa - t_b) + I_b, \quad \overline{I}_p = \kappa t_p(\kappa + t_p) + I_p \tag{12}$$

It is worth to note that the last term in d is an added flexural rigidity to the beam due to the induced electric field as previously mentioned.

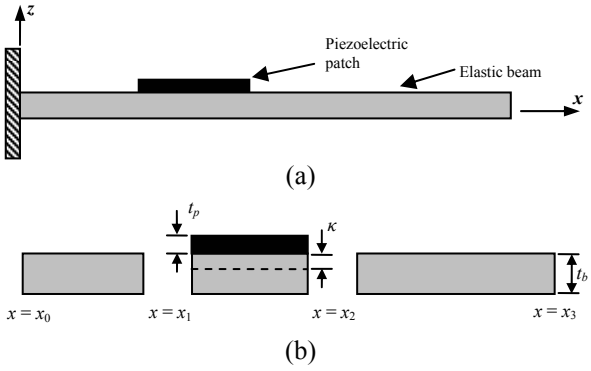

Fig. 1. a) Cantilever beam with piezoelectric patch
b) Segmentation of the beam

The third resulting electromechanical equation states that

$$\int_{x_1}^{x_2} (-e_{31} t_p u' + \alpha e_{31} w'' + \epsilon_{33}^{\varepsilon} \frac{\mathrm{V}}{t_p}) dx = -\int_S q dS \qquad (13)$$

The resulting boundary conditions of the piezoelectric layer at x_1 or x_2 are

$$\begin{aligned} & k u' + e_{31} A_p \frac{\mathrm{V}}{t_p} = 0, \quad \text{or} \quad u = 0 \\ & d w'' - \alpha e_{31} A_p \frac{\mathrm{V}}{t_p} = 0, \quad \text{or} \quad w' = 0 \\ & d w''' = 0, \quad \text{or} \quad w = 0 \end{aligned} \qquad (14)$$

Which represent the essential and natural boundary conditions required for applying the displacement and force continuity between at both ends of the middle region.

III. DISTRIBUTED TRANSFER FUNCTION

The equations of motion are first transformed to the Laplace domain. The transformed equations are cast into a state space form where the state vector is made of the deformation vector $D(x,s)$, and the strain vector $P(x,s)$ as follows [16]

$$Y_i(x,s) = \begin{Bmatrix} D(x,s) \\ P_i(x,s) \end{Bmatrix} \qquad (15)$$

Where

$$\begin{aligned} & D(x,s) = \{u_i, \quad w_i, \quad w_i'\}^T, \\ & P_i(x,s) = \{u_i', \quad w_i'', \quad w_i'''\}^T, \qquad i = 1,2,3 \end{aligned}$$

Where x and s are dropped from the variables for simplicity. The matrix equations of motion, in state space form, is given by

$$\frac{\partial}{\partial x} Y_i(x,s) = F_i(s) Y_i(x,s) \qquad (16)$$

Such that

$$F_i(s) = \begin{bmatrix} 0 & 0 & 0 & 1 & 0 & 0 \\ 0 & 0 & 1 & 0 & 0 & 0 \\ 0 & 0 & 0 & 0 & 1 & 0 \\ m_i s^2 / k_i & 0 & 0 & 0 & 0 & 0 \\ 0 & 0 & 0 & 0 & 0 & 1 \\ 0 & -m_i s^2 / d_i & 0 & 0 & 0 & 0 \end{bmatrix}$$

with $m_1 = m_3 = m$, $m_2 = m_b$, $k_1 = k_3 = k$, $k_2 = k_b$, $d_1 = d_3 = d$, $d_2 = d_b$

The boundary and displacement continuity conditions are cast in the following matrix equations

$$M_i Y_i(x_{i-1}, s) + N_i Y_i(x_i, s) = \gamma_i(s) \qquad (17)$$

Where

$$M_i = \begin{bmatrix} \mathbf{I} & \mathbf{0} \\ \mathbf{0} & \mathbf{0} \end{bmatrix}, \qquad N_1 = N_2 = \begin{bmatrix} \mathbf{0} & \mathbf{0} \\ \mathbf{I} & \mathbf{0} \end{bmatrix},$$

$$N_3 = \begin{bmatrix} k & 0 & 0 \\ 0 & d & 0 \\ 0 & 0 & d \end{bmatrix}$$

with $\mathbf{I}$ and $\mathbf{0}$ denoting 3×3 identity and zero matrices, respectively, and

$$\gamma_1(s) = \begin{Bmatrix} \mathbf{0} \\ D(x_1,s) \end{Bmatrix}, \quad \gamma_2(s) = \begin{Bmatrix} D(x_1,s) \\ D(x_2,s) \end{Bmatrix},$$

$$\gamma_3(s) = \begin{Bmatrix} D(x_2,s) \\ f \end{Bmatrix}, \quad f = \{0 \quad 0 \quad f_0\}^T$$

Similarly, the force continuity conditions of (14) can be cast in the following matrix form

$$\begin{bmatrix} B_1 & -B_2 & 0 & 0 \\ 0 & 0 & -B_2 & B_3 \end{bmatrix} \begin{Bmatrix} P_1(x_1,s) \\ P_2(x_1,s) \\ P_2(x_2,s) \\ P_3(x_2,s) \end{Bmatrix} = \begin{Bmatrix} \bar{\mathrm{V}} \\ \bar{\mathrm{V}} \end{Bmatrix} \qquad (18)$$

where

$$B_1 = B_3 = \begin{bmatrix} k_b & 0 & 0 \\ 0 & d_b & 0 \\ 0 & 0 & d_b \end{bmatrix}, \quad B_2 = N_3,$$

$$\bar{\mathrm{V}} = \frac{e_{31} A_p \mathrm{V}}{t_p} \begin{Bmatrix} 1 \\ -\alpha \\ 0 \end{Bmatrix}$$

The solution of the state space equation for each region is given by [17]

$$\begin{aligned} Y_i(x,s) &= \Psi_i(x,s) \gamma_i(s) \\ &= \begin{bmatrix} \Psi_i^{aa}(x) & \Psi_i^{ab}(x) \\ \Psi_i^{ba}(x) & \Psi_i^{bb}(x) \end{bmatrix} \gamma_i(s) \end{aligned} \qquad (19)$$

Where

$$\Psi_i(x,s) = e^{F_i x} \left[M_i e^{F_i x_{i-1}} + N_i e^{F_i x_i} \right]^{-1} \qquad (20)$$

With each of $\Psi_i^{pr}(p,r = a,b)$ as a 3×3 matrix that is made by partitioning of Ψ_i. Upon substitution of the definitions of Y_i and γ_i in (19) for the three regions, the following matrix equation can be formed at the common interfaces between the three regions

$$\begin{Bmatrix} P_1(x_1,s) \\ P_2(x_1,s) \\ P_2(x_2,s) \\ P_3(x_2,s) \end{Bmatrix} = \begin{bmatrix} \Psi_1^{bb}(x_1) & 0 \\ \Psi_2^{ba}(x_1) & \Psi_2^{bb}(x_1) \\ \Psi_2^{ba}(x_2) & \Psi_2^{bb}(x_2) \\ 0 & \Psi_3^{ba}(x_2) \end{bmatrix} \begin{Bmatrix} D(x_1,s) \\ D(x_2,s) \end{Bmatrix} \qquad (21)$$

substituting the last equation in (18), the result is the dynamic matrix equation of motion

$$K(s)\gamma_2(s) = \bar{F} \tag{22}$$

with

$$K(s) = \begin{bmatrix} B_1\Psi_1^{bb}(x_1,s) - B_2\Psi_2^{ba}(x_1,s) & -B_2\Psi_2^{bb}(x_1,s) \\ -B_2\Psi_2^{ba}(x_2,s) & B_3\Psi_3^{ba}(x_2,s) - B_2\Psi_2^{bb}(x_2,s) \end{bmatrix}$$

, $\bar{F} = \begin{Bmatrix} \bar{\mathrm{V}} \\ \bar{\mathrm{V}} \end{Bmatrix}$

IV. ELECTRICAL BOUNDARY CONDITIONS

As previously mentioned, obtaining OC and SC frequencies requires correct implementation of the electrical boundary conditions. For the SC condition, the voltage across the two piezoelectric electrodes vanishes, hence V = 0, and the dynamic equation of motion reduces to

$$K(s)\gamma_2(s) = 0 \tag{23}$$

In OC condition, the total surface charge, $\int_\Omega q d\Omega$, vanishes which reduces equation (13) to

$$\mathrm{V} = \frac{e_{31} t_p}{\epsilon_{33}^{\varepsilon}\,(x_2 - x_1)} \left(u\,|_{x_1}^{x_2} - \alpha w'\,|_{x_1}^{x_2} \right) \tag{24}$$

Which can be rewritten in the following matrix form

$$\bar{F} = -\bar{B}\gamma_2(s) \tag{25}$$

where

$$B_{oc} = \begin{bmatrix} a & 0 & -a\alpha \\ -a\alpha & d\alpha & a\alpha^2 \\ 0 & 0 & 0 \end{bmatrix} \quad a = \frac{e_{31}^2 t_p}{\epsilon_{33}^{\varepsilon}\,(x_2 - x_1)}$$

As a result, the last equation is substituted back in (22) resulting in a modified dynamic equation of motion

$$\left[K(s) + \bar{B} \right] \gamma_2(s) = 0 \tag{26}$$

Finally, the SC and OC frequencies are the values that force the determinant of the dynamic transfer matrix to vanish in both cases. Noting that $s = j\omega$, the characteristic equations for the SC and OC conditions can be written, respectively, as

$$\det\left[K(j\omega)\right] = 0 \;, \quad \det\left[K(j\omega) + \bar{B} \right] = 0 \tag{27}$$

V. MULTIPLE PIEZOELECTRIC ACTUATORS

The DTF solution is extended in this section to account for multiple piezoelectric actuators on a cantilever beam as shown.

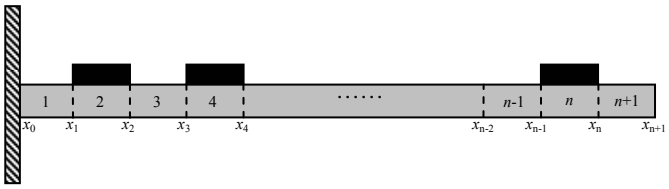

Fig. 2. beam with multiple piezoelectric patches

For n+1 segments, the force continuity conditions, equation (18), can be written in the following matrix form

$$\left[\mathbf{B}\right]\left\{\mathbf{P}\right\} = \left\{\mathbf{F}\right\} \tag{28}$$

Where

$$[\mathbf{B}] = \begin{bmatrix} B_1 & -B_2 & 0 & 0 & 0 & \cdots & & & 0 \\ 0 & 0 & -B_2 & B_3 & 0 & \cdots & & & 0 \\ \vdots & & & & \ddots & & & & \vdots \\ 0 & & & \cdots & 0 & B_{n-1} & -B_n & 0 & 0 \\ 0 & & & \cdots & 0 & 0 & 0 & -B_n & B_{n+1} \end{bmatrix},$$

$$[\mathbf{P}] = \begin{Bmatrix} P_1(x_1,s) \\ P_2(x_1,s) \\ \vdots \\ P_n(x_n,s) \\ P_{n+1}(x_n,s) \end{Bmatrix}, \quad [\mathbf{F}] = \begin{Bmatrix} \bar{V}_1 \\ \bar{V}_2 \\ \vdots \\ \bar{V}_{n-1} \\ \bar{V}_n \end{Bmatrix}$$

Similarly, (21) can be extended for the n+1 segments and rewritten as follows

$$\left\{\mathbf{P}\right\} = \left[\mathbf{\Psi}\right]\left\{\mathbf{D}\right\} \tag{29}$$

Such that

$$[\mathbf{\Psi}] = \begin{bmatrix} \Psi_1^{bb}(x_1,s) & 0 & \cdots & & 0 \\ \Psi_2^{ba}(x_1,s) & \Psi_2^{bb}(x_1,s) & & & \\ \vdots & & \ddots & & \vdots \\ & & & \Psi_n^{ba}(x_n,s) & \Psi_n^{bb}(x_n,s) \\ 0 & & \cdots & & \Psi_{n+1}^{ba}(x_n,s) \end{bmatrix}$$

$$[\mathbf{D}] = \begin{Bmatrix} D(x_1,s) \\ D(x_2,s) \\ \vdots \\ D(x_{n-1},s) \\ D(x_n,s) \end{Bmatrix}$$

Substituting equation (29) in (28), the dynamic matrix equation of motion for n+1 segments reads

$$\left[\mathbf{K}\right]\left\{\mathbf{D}\right\} = \left\{\mathbf{V}\right\} \tag{30}$$

where $\left[\mathbf{K}\right] = \left[\mathbf{B}\right]\left[\mathbf{H}\right]$ is the dynamic "stiffness" transfer matrix. For the OC condition, the following matrix equation is obtained from the voltage across the electrodes of all the piezoelectric patches

$$\{\mathbf{V}\} = \left[\mathbf{B^{oc}}\right]\{\mathbf{D}\} \tag{31}$$

where

$$\left[\mathbf{B^{oc}}\right] = \begin{bmatrix} -B_1^{oc} & B_2^{oc} & 0 & \cdots & 0 \\ -B_1^{oc} & B_2^{oc} & 0 & \vdots & \vdots \\ 0 & 0 & \ddots & 0 & 0 \\ \vdots & \cdots & 0 & -B_{n-1}^{oc} & B_2^{oc} \\ 0 & \cdots & 0 & -B_{n-1}^{oc} & B_n^{oc} \end{bmatrix}$$

Finally, combining the last two equation together results in the global equation of motion required to solve for the OC frequencies of the system

$$\left(\left[\mathbf{K}\right] - \mathbf{B^{oc}}\right)\{\mathbf{D}\} = \{\mathbf{0}\} \tag{32}$$

VI. RESULTS

The modal Effective Electromechanical Coupling Coefficient (EMCC) is known as a critical parameter in justifying the performance of piezoelectric materials since it describes the efficiency of converting mechanical strain to electric charges and vice versa. For a vibrating structure, the modal EMCC for mode r, k_r^2, is defined by [9]

$$k_r^2 = \frac{(\omega_r^{oc})^2 - (\omega_r^{sc})^2}{(\omega_r^{sc})^2} \tag{33}$$

Where ω^{oc} and ω^{sc} are the natural frequencies of the structure under the OC and SC boundary conditions for the rth mode.

For validation of the proposed analytical solution, consider a miniature 2.7-cm cantilever beam that has E_b = 100 GPa, ρ_b = 8400 kg/m3 and t_b = 1 mm. The left end (x_1) of the piezoelectric patch is 0.5-mm away from the fixed end of the beam with t_p = 0.178 mm, ρ_p = 7800 kg/m^3, C_{11}^E=62 GPa, e_{31}= -19.84 C/m^2 and $\epsilon_{33}^{\varepsilon}$ = 33.64 nF/m. As can be seen in Table 1, the natural frequencies obtained by the current DTF method are identical to the ones obtained by the exact, time-separable, solution of the differential equation [10].

A parametric analysis has been performed to optimize the length and thickness ratios of the piezoelectric patch for maximum modal EMCC. It can be seen that the optimum parameters are dependable on the mode number. For the first mode a maximum EMCC of 0.05 is obtained when the thickness of the piezoelectric patch is half that of the beam, and its coverage ratio is about half the length of the beam. As for the second mode, a max EMCC of 0.029 occurs for the highest thickness and length ratios of the piezoelectric patch.

TABLE I.
OC / SC natural frequencies and modal EMCC: Analytical vs. DTF

	Mode 1			Mode 2		
	ω^{sc}	ω^{oc}	k^2(%)	ω^{sc}	ω^{oc}	k^2(%)
Analytical	116.01	116.28	0.45	586.70	586.70	0.43
DTF	116.01	116.28	0.45	587.96	587.96	0.43

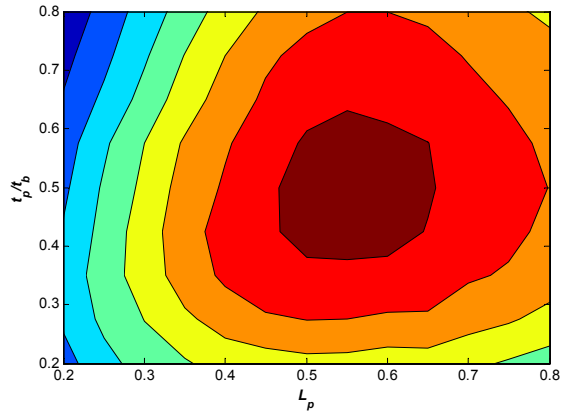

(a)

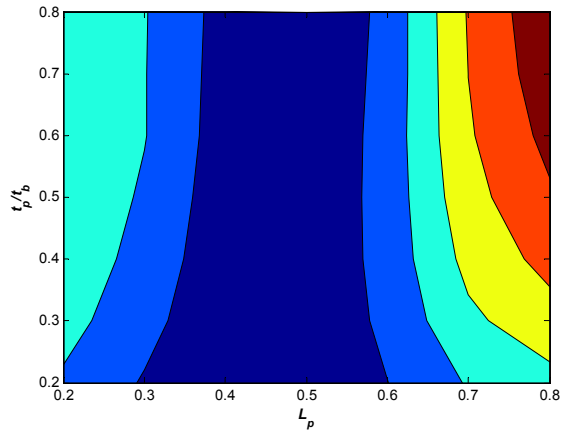

(b)

Fig. 3. Variation of the EMCC with piezoelectric patch thickness and length ratios a) 1st mode b) 2nd mode

VII. CONCLUSION

The current modeling approach of the free vibrations of piezoelectric structures is systematically simple and requires no previous assumption of the solution type. Noting that the definition of EMCC is very sensitive to frequency predictions, the DTF method under consideration is of special interest in the design of piezoelectric energy harvesting devices since the exact frequencies can be easily calculated, leading to exact determination of the modal EMCC which is an ultimate design parameter. Parametric analysis can be easily performed then to optimize the size of the piezoelectric patch which was shown to be dependent on the resonance mode of vibration.

REFERENCES

[1] Lu F, Lee H P and Lim S P 2004 Modeling and analysis of micro piezoelectric generators for micro-electromechanical-systems applications *Smart Mater. Struct.***13** 57-63

[2] Bailey T and Hubbard J E Jr 1985 Distributed piezoelectric polymer active vibration control of a cantilever beam *J. Guidance Control Dyn.* **8** 605–11

[3] Crawley E F and de Luis J 1987 Use of piezoelectric actuators as elements of intelligent structures *AIAA J.* **25** 1373–85

[4] Hagood N, Chung W and von Flatow A 1990 Modeling of piezoelectric actuator dynamics for active structural control *J. Intell. Mater. Syst. Struct.* **1** 327–54

[5] Benjeddou A 2000 Advances in piezoelectric finite elements modeling of adaptive structural elements: a survey *Comput. Struct.* **74** 465–76

[6] Tong L and Luo Q 2003 Exact dynamic solutions to piezoelectric smart beams including peel stresses I: theory and application *Int. J. Solids Struct.* **40** 4789–4812

[7] Erturk A and Inman D J 2008 A distributed parameter electromechanical model for cantilevered piezoelectric energy harvesters *J. Vibrat. Acoust.* **127** doi: 10.1115/1.2890402

[8] Maurini C, Porfiri M and Pouget J 2006 Numerical methods for modal analysis of stepped piezoelectric beams *J. Sound Vib.* **298** 918-933

[9] Burmann P, Raman A and Garimella S V 2002 Dynamics and topology optimization of piezoelectric fans *IEEE Trans. Compon. Packag. Manuf. Technol. Part A* **25** 592–600

[10] Basak S, Raman A and Garimella S V 2005 Dynamic response optimization of piezoelectrically excited thin resonant beams *J. Vibrat. Acoust.* **127** 18-27

[11] Maxwell N D and Asokanthan S F 2004 Modal characteristics of a flexible beam with multiple distributed actuators *J. Sound Vib.* **269** 19-31

[12] Pestel E C and Leckie F A 1963 *Matrix Methods in Elastomechanics* (New York: McGraw-Hill)

[13] Baz A 2001 Active control of periodic structures *J. Vibrat. Acoust.* **123** 472-479

[14] Singh A, Pines D J and Baz A 2004 Active/passive reduction of vibration of periodic one-dimensional structures using piezoelectric actuators *Smart Mater. Struct.***13** 698-711

[15] Ruzzene M and Scarpa F 2003 Control of wave propagation in sandwich beams with auxetic core *J. Intell. Mater. Syst. Struct.* **14** 443-453

[16] Yang B and Tan C A 1992 Transfer functions of one-dimensional distributed parameter systems *J. Appl. Mech.* **59** 1009-1014

[17] Yang B 1994 Distributed transfer function analysis of complex distributed parameter systems *J. Appl. Mech.* **61** 84-92

[18] Benjeddou A, Trindade M A and Ohayon R 1997 A unified beam finite element model for extension and shear piezoelectric actuation mechanisms *J. Intell. Mater. Syst. Struct.* **8** 1012-1025